

# Functional connectivity abnormalities and associated cognitive deficits in fetal alcohol Spectrum disorders (FASD)

Jeffrey R. Wozniak<sup>1</sup> · Bryon A. Mueller<sup>1</sup> · Sarah N. Mattson<sup>3</sup> · Claire D. Coles<sup>4</sup> · Julie A. Kable<sup>4</sup> · Kenneth L. Jones<sup>5</sup> · Christopher J. Boys<sup>1</sup> · Kelvin O. Lim<sup>1</sup> · Edward P. Riley<sup>3</sup> · Elizabeth R. Sowell<sup>2</sup> · the CIFASD

Published online: 12 October 2016  
© Springer Science+Business Media New York 2016

**Abstract** Consistent with well-documented structural and microstructural abnormalities in prenatal alcohol exposure (PAE), recent studies suggest that functional connectivity (FC) may also be disrupted. We evaluated whole-brain FC in a large multi-site sample, examined its cognitive correlates, and explored its potential to objectively identify neurodevelopmental abnormality in individuals without definitive dysmorphic features. Included were 75 children with PAE and 68 controls from four sites. All participants had documented heavy prenatal alcohol exposure. All underwent a formal evaluation of physical anomalies and dysmorphic facial features. MRI data were collected using modified matched protocols on three platforms (Siemens, GE, and Philips). Resting-state FC was examined using whole-brain graph theory metrics to characterize each individual's connectivity. Although whole-brain FC metrics did not discriminate prenatally-exposed from unexposed overall, atypical FC ( $> 1$  standard deviation from the grand mean) was significantly more common (2.7 times) in the PAE group vs. controls. In a subset of 55 individuals (PAE and controls) whose dysmorphology examination could not definitively characterize them as either

Fetal Alcohol Syndrome (FAS) or non-FAS, atypical FC was seen in 27 % of the PAE group, but 0 % of controls. Across participants, a 1 % difference in local network efficiency was associated with a 36 point difference in global cognitive functioning. Whole-brain FC metrics have potential to identify individuals with objective neurodevelopmental abnormalities from prenatal alcohol exposure. When applied to individuals unable to be classified as FAS or non-FAS from dysmorphology alone, these measures separate prenatally-exposed from non-exposed with high specificity.

**Keywords** Fetal alcohol (FAS, FASD) · Brain · Functional MRI (fMRI), resting-state, connectivity · Neuropsychology

## Introduction

Fetal Alcohol Spectrum Disorders (FASD) are associated with a wide range of underlying neuroanatomical abnormalities as seen with Magnetic Resonance Imaging (MRI) (Riley et al. 2004). From the earliest studies, it has been clear that the backbone of the brain's functional network - the white matter - is impacted by prenatal alcohol exposure (PAE). Studies demonstrated that complete corpus callosum agenesis can occur and also highlighted other more common abnormalities including thinning, hypoplasia, and partial agenesis (Riley et al. 1995). Volumetric MRI studies show that PAE is associated with widespread abnormalities in white matter macrostructure throughout the brain (Archibald et al. 2001). Diffusion Tensor Imaging (DTI) has demonstrated white matter pathology in PAE, highlighting microstructural abnormalities in regions using multiple methodologies (Donald et al. 2015a, b; Fan et al. 2015; Fryer et al. 2009; Lebel et al. 2010; Lebel et al. 2008; Ma et al. 2005; Sowell et al. 2008; Sowell et al. 2010; Taylor et al. 2015; Wozniak et al. 2006; Wozniak

✉ Jeffrey R. Wozniak  
jwozniak@umn.edu

the CIFASD

<sup>1</sup> Department of Psychiatry, University of Minnesota Twin Cities, F282/2A West, 2450 Riverside Ave, Minneapolis, MN 55454, USA

<sup>2</sup> Children's Hospital of Los Angeles, University of Southern California, Los Angeles, CA, USA

<sup>3</sup> San Diego State University, San Diego, CA 92182, USA

<sup>4</sup> Emory University, Atlanta, GA 30322, USA

<sup>5</sup> University of California, San Diego, La Jolla, CA 92093, USA

et al. 2009). These abnormalities have clinical relevance, evidenced by their association with cognitive disturbances (Fan et al. 2015; Malisza et al. 2012; Sowell et al. 2008; Spottiswoode et al. 2011; Wozniak et al. 2009). Related diffusion techniques, such as quantitative susceptibility mapping, have shown similar microstructural abnormalities in a mouse model of PAE (Cao et al. 2014).

Several studies have demonstrated that white matter macro- and micro-structural abnormalities in PAE are also reflected in functional connectivity (FC) disturbances, using both task-based functional MRI (fMRI) and resting-state FC methods. Wozniak et al. (2011) showed inter-hemispheric FC disturbances in PAE corresponding to microstructural abnormalities (from DTI-tractography), notably in the posterior aspect of the callosum. In that study, atypical inter-hemispheric FC was reflected in significantly lower correlations between fMRI signal in right and left para-central cortical regions (regions predominantly inter-connected by posterior callosal projection fibers). Inter-hemispheric FC abnormalities of this type may be evident as early as infancy (Donald et al. 2016). Taking a different approach, Santhanam et al. (2011) examined the default mode network in PAE - comprising medial prefrontal cortex, posterior cingulate, pre-cuneus, inferior parietal, and medial temporal regions. In that study, the expected network “deactivation” upon starting an arithmetic task was abnormal in prenatally-exposed adults. That study highlighted dysfunction in the normal coordinating process of alternating the resting-state network and various “active” cognitive networks. Another resting-state FC study in PAE demonstrated abnormalities in whole-brain connectivity, using graph theory metrics similar to those utilized in the current study (Wozniak et al. 2013). Finally, other task-based fMRI studies have also revealed FC abnormalities in PAE, including alterations in fronto-striatal coupling (Roussotte et al. 2012).

FC represents the brain’s capacity for real-time coordination of activity across both time and distance. In resting-state FC studies, correlations in fMRI data are used to “map” brain networks based on patterns of synchronized activity (Biswal et al. 1995). In contrast to “task-based” networks related to attention, executive functioning, or stimulus salience for example, resting-state networks may be involved in non-task, off-line activities including memory consolidation and planning (Raichle and Snyder 2007). From a network analysis perspective, functional brain activity appears to fit “small world network” parameters well (Bassett and Bullmore 2006). Small world networks have highly clustered, modular processing “centers” – along with a few highly efficient long-distance communication “paths” (Rubinov and Sporns 2010). In a small world network, each node (brain region) is densely connected with its neighboring regions (clustering), but long-distance communication is enhanced by a few “trunk-lines”

that facilitate efficient jumps between distant regions without traversing the many intervening nodes (Watts and Strogatz 1998). In the brain, white matter provides these highly efficient routes between distant grey matter regions where more modular/clustered processing occurs.

Graph theory provides a set of robust metrics for evaluating the properties of small-world networks (Achard and Bullmore 2007). One advantage of applying these methods to the study of a clinical condition like PAE is that each individual’s network status can be specifically characterized – allowing for analyses at both the group level and the individual level. The ability to identify individual functional network pathology could be valuable in PAE – a condition for which there is substantial heterogeneity in presentation. For example, dysmorphic facial features are only present in a portion of affected individuals who show cognitive deficits, complicating the diagnosis of FASD (Green et al. 2009; Jacobson 1998; Mattson et al. 1997). The ability to characterize an individual’s functional connectivity as “typical” or “atypical” could potentially be harnessed in the search for better diagnostic tools. Furthermore, examining relationships between individual network connectivity and cognitive functioning will add to the overall understanding of how alcohol exposure manifests clinically. In a previous small study examining graph theory connectivity metrics in FASD, Wozniak et al. (2013) found preliminary trend-level associations between FC and neurocognitive functioning – including verbal memory and executive functioning; other studies have demonstrated associations between functional connectivity and intelligence in children (Wu et al. 2013).

The current study (which does not contain any of the same participants as Wozniak et al. 2013), is comprised of data collected at four sites in the Collaborative Initiative on Fetal Alcohol Spectrum Disorders (CIFASD). It utilized whole brain FC methods in a large sample, seeking to extend the understanding of brain-cognition relationships in PAE. The rationale for examining whole-brain FC in this study is based on the following: 1) the effects of alcohol on the developing brain have been shown to be widespread rather than discrete; 2) there is value in characterizing the overall severity of brain effects of PAE; and 3) measures of global brain functioning may ultimately have utility in addressing diagnostic challenges and as outcome measures in FASD intervention studies.

Based on what is known about the widespread effects of PAE on both grey and white matter development, we hypothesized that global cortical FC would be disturbed in children and adolescents with PAE. Low network efficiency and evidence of disconnectivity were predicted. Summary measures of network connectivity were expected to correlate with cognitive functioning including components of IQ, memory, and executive functioning. In all cases, we expected to see low network efficiency and poor overall connectivity to be associated with greater cognitive impairment.

## Methods

### Participants

Background information about the CIFASD project is available in a separate publication (S. N. Mattson et al. 2010) and at [www.cifasd.org](http://www.cifasd.org). For the current study, participants were recruited from four CIFASD sites (Los Angeles, San Diego, Minneapolis, Atlanta) between 2012 and 2014. Prenatal alcohol exposure histories were obtained through retrospective maternal report or social service, legal, or medical records. Participants were included in the PAE group if there was a history of heavy prenatal alcohol exposure (>13 drinks/week or >4 drinks/occasion during pregnancy) or when such exposure was suspected in a child with an FAS diagnosis. In many cases, detailed history about exposure amounts or patterns of exposure was unattainable; children were considered to have heavy prenatal alcohol exposure if mothers were known to be “alcoholic” or alcohol-abusing during pregnancy. In all cases, alcohol was the predominant substance of abuse. Participants were included in the non-exposed control group if there was a reliable history of only minimal (<1 drink/week, never >2 drinks/occasion) or no exposure in pregnancy.

The majority of participants (PAE and controls) were evaluated using a standardized dysmorphology examination conducted by the CIFASD Dysmorphology Core (KLJ). Based on criteria outlined previously (Kenneth Lyons Jones et al. 2006; Sarah N. Mattson et al. 2010), the evaluation resulted in a determination of 1) Fetal Alcohol Syndrome (FAS); 2) non-FAS; or 3) a “deferred” status due to some criteria being met, but not enough to diagnose FAS. FAS was diagnosed on the basis of two or more of the following key facial features: thin vermilion border, smooth philtrum, and short palpebral fissure length – together with either microcephaly (occipital-frontal circumference  $\leq 10\%$ ) or growth deficiency (height or weight  $\leq 10\%$ ) or both. The deferred status was applied when an individual had A.) One key dysmorphic facial feature as described above or B.) Microcephaly and growth deficiency, or C.) Microcephaly or growth deficiency and one additional minor non-facial physical malformation (railroad track ear, hockey stick palmar crease, etc.). A significant number of individuals without PAE (i.e. controls) received a “deferred” classification – highlighting the fact that the presence of one dysmorphic feature is relatively common and not diagnostic in and of itself (K. L. Jones et al. 2010).

Additional exclusion criteria for all subjects were another developmental disorder (ex. Autism), very low birthweight (<1500 g), traumatic brain injury (including head injury with loss of consciousness >30 min), other medical condition affecting the brain (ex. Epilepsy), severe psychiatric disability that would prevent participation (ex. psychosis or mania), substance use by the participant, English as a second

language, international adoption after age 5 or within 2 years of study visit, or contraindications to MRI scanning.

Control participants were excluded for parent-reported history of prenatal substance exposure and for diagnosed psychiatric conditions. Parents or caregivers of all participants were administered the Diagnostic Interview Schedule for Children-IV (C-DISC-4.0; (Shaffer et al. 2000)). Because pre-screening was utilized during recruitment, the DISC data for enrolled participants revealed only minimal parent-reported symptoms in the control group (2 controls had ADHD symptoms, 5 had Oppositional Defiant symptoms, and 3 had Conduct Disorder symptoms; no controls had anxiety or depressive symptoms or other major psychiatric symptoms). Psychiatric co-morbidity was not an exclusion criterion for participants with PAE because it is well-recognized that co-morbidity is high in FASD (Streissguth and O’Malley 2000). Based on the C-DISC-IV data, 54 participants in the PAE group had ADHD symptoms, 34 had Oppositional Defiant symptoms, 13 had Conduct Disorder symptoms, 6 had anxiety disorder symptoms, and 4 had depressive disorder symptoms.

Participants were 7–17 year old at the time of neurocognitive evaluation and MRI scanning. The vast majority of participants completed the neurocognitive evaluation and MRI on the same day. In a few cases, they were separated by a few days or weeks. A total of 165 participants (87 with PAE & 78 Controls) met inclusion criteria. Table 1 contains the demographics for the participants who were included in the analyses after eliminating those with excessive movement and incomplete networks (see results for complete description).

All participants underwent an Institutional Review Board (IRB)-approved informed consent process involving a parent or guardian as well as a separate assent process with the child. All study procedures were approved by the IRBs at each of the four sites. Participants were compensated for their time.

### Neurobehavioral evaluation

Primary caregivers were administered specific modules from the C-DISC-4, a computerized structured interview based on the DSM-IV (Shaffer et al. 2000). Neuropsychological testing was conducted during one or two sessions by trained research assistants who were blind to exposure status. Quality control methods included a video review of test administration procedures and a scoring check for every 10th administration. From a larger battery of neuropsychological measures administered in CIFASD, specific measures were chosen for analyses here based on domains that showed relationships with FC in previous studies. These include the Differential Ability Scales – Second Edition (DAS-II) (Elliott 2007), the California Verbal Learning Test – Children’s Edition (CVLT-C) (Delis et al. 1994), the Delis-Kaplan Executive Functioning System (D-KEFS) (Delis et al. 2001), and the NEPSY-II Developmental Neuropsychological Assessment (Korkman et al. 2007).

**Table 1** Demographic characteristics of participants included in analyses

	PAE (n = 75)	Control (n = 68)	Statistical Test
Age [M (SD)]	12.7 (2.5)	13.8 (2.4)	$t(141) = -2.66, p = .009$
Sex [n (%Female)]	34 (45 %)	35 (52 %)	$\chi^2 = .54, p = .505$
Race [n (%White)]	51 (68 %)	43 (63 %)	$\chi^2 = .34, p = .599$
Ethnicity [n (%Hispanic)]	13 (17 %)	9 (13 %)	$\chi^2 = .80, p = .672$
Handedness [n (%Right)]	66 (88 %)	58 (85 %)	$\chi^2 = 1.18, p = .759$
Fetal Alcohol Syndrome Diagnosis [n (%)]	12 (17 %)	0 (0 %)	$\chi^2 = 22.1, p < .001$
Physical manifestations			
<sup>A</sup> Growth Deficiency	18 (24 %)	5 (7 %)	$\chi^2 = 9.92, p = .007$
<sup>B</sup> Microcephaly	14 (19 %)	0 (0 %)	$\chi^2 = 16.58, p < .001$
<sup>C</sup> Dysmorphic Face	28 (37 %)	8 (11 %)	$\chi^2 = 14.09, p = .001$
Site [n]			
Los Angeles	16 (21 %)	14 (21 %)	
San Diego	20 (27 %)	15 (22 %)	
Minneapolis	25 (33 %)	29 (43 %)	
Atlanta	14 (19 %)	10 (14 %)	

Shown here are 143 participants included in the analyses only. Of the initial eligible pool of 165 participants, 20 participants (12 with PAE and 8 controls) were eliminated for excessive motion during MRI; an additional 2 controls were eliminated for networks that did not completely connect within the cost parameters set for the study

PAE Prenatal Alcohol Exposure group

<sup>A</sup> Height or weight  $\leq$  10%ile

<sup>B</sup> Head circumference  $\leq$  10%ile

<sup>C</sup> At least two of the following: Palpebral Fissure Length  $\leq$  10%ile, thin vermilion border, smooth philtrum (4 or 5 on lipometer scale)

## MRI acquisition procedures

MRI data were acquired at four sites on scanners from three vendors: Children's Hospital of Los Angeles (Philips Achieva); University of California – San Diego (General Electric MR750); University of Minnesota and Emory University (both Siemens Tim Trio). Acquisition sequences were modeled on protocols developed for multi-site imaging by the Pediatric Imaging Neurocognition and Genetics (PING) group (Table 2) (<http://ping.chd.ucsd.edu>). The sequence included high resolution T1-weighted images, a T2-weighted set, 30-direction DTI, and gradient-echo EPI scans for resting-state fMRI. The acquisition parameters in Table 2 are just those for data examined in the current set of analyses (T1 and fMRI). Participants were not sedated for the MRI scan nor were their usual medications modified. During the resting-state fMRI scan, participants were instructed to close their eyes and remain still. Table 2 contains details of the acquisition sequences by site.

## MRI processing

### T1 cortical parcellation

Cortical parcellation of the T1 volume was performed using FreeSurfer version 5.3.0 ([surfer.nmr.mgh.harvard.edu](http://surfer.nmr.mgh.harvard.edu)) (Dale et al. 1999) and the default Desikan-Killiany atlas. Processing

included removal of non-brain tissue, automated Talairach transformation, segmentation, intensity normalization, tessellation of the grey matter / white matter boundary, topology correction, surface deformation, and automated parcellation of the cortical grey matter into 34 ROIs per hemisphere. Each subject's data was visually inspected by a trained operator to ensure accuracy of the cortical parcellation, but manual editing was not employed.

### Resting-state fMRI processing

fMRI data processing was carried out using the FEAT tool from the FMRIB Software Library (FSL) version 5.0.7 (<http://fsl.fmrib.ox.ac.uk/fsl/fslwiki/>) (Smith et al. 2004; Woolrich et al. 2009). The following pre-statistics processing was applied: motion correction, brain extraction, spatial smoothing (6 mm FWHM), grand-mean intensity normalization, and high pass temporal filtering ( $\sigma = 50$ s). Correction for geometric distortion caused by magnetic field inhomogeneity was carried out on a subset of data: those data that were collected along with a reverse phase-encoded gradient echo fMRI scan acquired for this purpose (all Minnesota data and a subset of the Atlanta data). ICA-based data analysis was also carried out during the FEAT processing step using the FSL tool MELODIC. The FSL tool `fsl_fix` was then used to perform automated ICA de-noising of the fMRI data.



**Table 2** MRI sequence and parameters

Platform	Sequence	Imaging parameters	Purpose
Philips (Los Angeles)			
	T1-weighted MPRAGE	TR = 6.8 ms, TE = 3.2 ms, TI = 845 ms, 170 slices, voxel size = 1x1x1.2 mm, FOV = 256 mm, flip angle = 8 degrees	Segmentation & cortical parcellation
	Resting fMRI	TR = 2500 ms, TE = 30 ms, 50 ascending slices, no skip, voxel size = 2.67 × 2.67x3mm, FOV = 256 mm, flip angle = 75 degrees, 156 or 232 measures*	Measurement of BOLD signal
San Diego (General Electric)			
	T1-weighted IRSPGR	TR = 7.38 ms, TE = 2.984 ms, TI = 640 ms, 166 slices, voxel size = 0.94 × 0.94 × 1.2 mm, FOV = 240 mm, flip angle = 8 degrees	Segmentation & cortical parcellation
	Resting fMRI	TR = 2000 ms, TE = 30 ms, 33 interleaved slices, no skip, voxel size = 3.4 × 3.4x4mm, FOV = 220 mm, flip angle = 75 degrees, 180 measures	Measurement of BOLD signal
Siemens (Minnesota & Atlanta)			
	T1-weighted MPRAGE	TR = 2170 ms, TE = 4.33 ms, TI = 1100 ms, 192 slices, voxel size = 1x1x1mm, FOV = 256 mm, flip angle = 7 degrees	Segmentation & cortical parcellation
	Resting fMRI	TR = 2000 ms, TE = 30 ms, 33 interleaved slices, 1 mm skip, voxel size = 3.4 × 3.4x4mm, FOV = 220 mm, flip angle = 75 degrees, 180 measures.	Measurement of BOLD signal

\*A total of 21 subjects underwent a single resting-state fMRI run of 156 volumes. An additional 9 subjects underwent two consecutive resting-state fMRI runs of 116 volumes each, which were ultimately concatenated

Registration of the T1 volume to the fMRI data was performed using the FreeSurfer tool *bbregister* (Greve and Fischl 2009). White matter and CSF masks were created on the fMRI data by registering the bilateral FreeSurfer lateral ventricle and white matter ROIs using the *bbregister*-determined transform applied using the FSL tool *FLIRT*. Timecourses from the CSF and white matter ROIs along with the six motion parameters were then used as voxel-wise nuisance regressors in processing the fMRI data with the FSL tool *film\_gls*. To further reduce artifactual correlations within the fMRI data, volume scrubbing was applied to the data using methods outlined in Power et al. (2012).

#### Time-series extraction

The 68 FreeSurfer cortical ROIs (34 per hemisphere) were registered to the processed fMRI data using *bbregister*. The parcellations were dilated during registration, but none were allowed to overlap and voxels outside the brain-mask were excluded. ROIs that contained fewer than 10 fMRI voxels for any participant were excluded from the final analysis. This resulted in the exclusion of 6 ROIs (bilateral entorhinal, frontal pole and temporal pole), leaving a total of 62 ROIs (31 per hemisphere). The mean fMRI time-series of all voxels within each ROI were then extracted for each participant.

#### Computation of the network metrics

Pearson correlations were computed between the time-series from all possible pairs of the 62 cortical ROIs using

MATLAB (Mathworks, Natick, MA). Graph theory network metrics were computed for each subject's Pearson correlation matrix (Bullmore and Sporns 2009; Rubinov and Sporns 2010) utilizing tools from the BCT toolbox (<http://sites.google.com/a/brain-connectivity-toolbox.net/bct/Home>). Cortical ROIs served as network nodes and correlation values served as the connections (edges). The cost of a network is defined as the ratio of existing connections to the total number of possible connections in the graph  $((62 \times 61) / 2 = 1891$  for a 62 node network). Binary, non-weighted and non-directional adjacency matrices were determined by applying a participant-specific threshold to each participant's data across a range of costs from 0.1 to 0.5, with 0.05 step increments. Four metrics of interest were derived: *characteristic path length*, *mean clustering coefficient*, *local efficiency* and *global efficiency* (Latora and Marchiori 2001; Watts and Strogatz 1998).

Path length is the smallest number of connections that must be traversed to connect any pair of nodes in the network. The *characteristic path length* (CPL) is the average *path length* between all pairs of nodes in the network. A higher than normal CPL implies less reliance on highly efficient "trunk-lines" for long distance communication and more reliance on multiple smaller "jumps" between regions. The *mean clustering coefficient* (MCC) reflects the density of local connections. *Global efficiency* (GLOB), inversely related to path length, reflects properties of the network associated with long-range connections that facilitate rapid communication between remote brain regions; it is thought to reflect the network's capacity for parallel information propagation and processing. In

contrast, *local efficiency* (LOC) is thought to reflect properties of the network associated with modular processing within more localized brain regions (Latora and Marchiori 2001).

In network graph mathematics, cost has implications for overall topography of the network and there are multiple costs at which the network metrics can be examined. We examined the networks at a cost at which all participants had fully-connected networks. A fully-connected network contains at least one possible pathway between every node.

### Statistical analyses

Demographic data were tested for group differences using independent-samples t-tests and chi-square analyses. T-tests and chi-square analyses tested for differences between participants who were included in the study vs those who were excluded. T-tests were used to test for differences in motion parameters between the PAE group and controls. Prior to the primary analyses, a number of potential confounding factors were examined by testing for group differences using ANOVA. If no significant group differences were found across levels of the potentially confounding variable, the variable was not controlled for in subsequent analyses. Primary analyses comparing groups (PAE vs. control) on network connectivity measures consisted of independent samples t-tests. The impact of multiple comparisons was addressed with Benjamini and Hochberg False Discovery Rate (FDR) correction (Benjamini and Hochberg 1995). A multiple ANOVA was utilized to test for group differences (PAE vs. control) in neurocognitive functioning. Lastly, Pearson correlations were used to directly examine relationships between network connectivity metrics and performance on neurocognitive tests.

## Results

### Participants eliminated for excessive motion during MRI

A total of 20 participants were excluded from the analyses reported here because of excessive motion in 30 % or more of the volumes. The excluded participants were as follows: 12 PAE and 8 Controls; 14 male and 6 female; 7 from Los Angeles, 6 from San Diego, 3 from Minneapolis, 4 from Atlanta. Among the included participants, there was not a significant difference in *relative* root mean square (RMS) translation between the PAE group ( $m = .082$ ,  $sd = .037$ ) and the control group ( $m = .072$ ,  $sd = .032$ ), [ $t(141) = 1.44$ ,  $p = .153$ ]. There was also not a significant difference in *absolute* RMS translation between the PAE group ( $m = .505$ ,  $sd = 1.12$ ) and control group ( $m = .450$ ,  $sd = .713$ ), [ $t(141) = .349$ ,  $p = .728$ ]. Furthermore, there was not a significant difference in volumes rejected because of motion

between the PAE group ( $m = 11.4$  volumes,  $sd = 14.1$ ) and the control group ( $m = 9.1$  volumes,  $sd = 12.9$ ), [ $t(141) = 1.00$ ,  $p = .319$ ].

### Participants eliminated for less-than-fully connected networks

Of the participants who had motion within the allowable range, 2 (both controls) had networks that did not fully connect at a cost of .30 or below and were excluded as a result. At costs above 0.30, numerous subjects' networks no longer retained small world properties ( $\sigma < 1.5$ ) (Bassett and Bullmore 2006). The remaining sample comprised 143 participants with analyzable fMRI data (75 PAE, 68 Controls).

### Testing for differences between included and excluded participants

Several analyses were conducted to determine how participants who were excluded for motion or for having un-connected networks ( $n = 22$ ) differed from included participants ( $n = 143$ ). There was a significant difference in age between included ( $m = 13.2$  years,  $sd = 2.52$ ) and excluded ( $m = 11.9$  years,  $sd = 2.6$ ) participants [ $t(163) = 2.21$ ,  $p = .029$ ]. There was not a difference between included and excluded participants in sex [ $\chi^2 = 2.07$ ,  $p = .112$ ], race [ $\chi^2 = 5.07$ ,  $p = .534$ ], ethnicity [ $\chi^2 = 3.59$ ,  $p = .166$ ], history of prenatal alcohol exposure [ $\chi^2 = .034$ ,  $p = .854$ ], FAS Diagnosis [ $\chi^2 = .025$ ,  $p = .988$ ], nor DAS General Conceptual Ability [ $t(161) = 1.56$ ,  $p = .120$ ].

### Testing for confounding factors

After eliminating those with obvious excessive motion, participant motion during fMRI can still lead to spurious correlations in voxel intensity, even after the processing stream is applied (motion correction followed by regression against the CSF, WM, and six motion timecourses). In order to test for a potential confounding influence of motion, Pearson correlations were computed between the number of fMRI volumes that were rejected because of motion and the network metrics of interest. None of these correlations was significant: (CPL =  $-.11$ ,  $p = .21$ ; MCC =  $-.05$ ,  $p = .60$ ; GLOB =  $-0.1$ ,  $p = .96$ ; LOC =  $-.10$ ,  $p = .15$ ). For this reason, the motion correction parameters were not entered as covariates in any of the remaining statistical analyses. As indicated above, motion was regressed out as part of the pre-processing.

Age was also considered as a potential confounding factor to the network metrics because some studies have shown age-related resting-state FC patterns (Fair et al. 2009). Pearson correlations were computed between age and the network metrics, but none were significant (CPL =  $.06$ ,  $p = .49$ ; MCC =  $-.07$ ,  $p = .43$ ; GLOB =  $-.08$ ,  $p = .32$ ; LOC =  $-.10$ ,  $p = .22$ ). Therefore, age was not included as a covariate.

Collection site (Los Angeles, San Diego, Minnesota, Atlanta) was also examined as a potential confounding factor. ANOVAs revealed no significant site effects for any of the four network metrics (CPL:  $F(3139) = .38, p = .77$ ; MCC:  $F(3139) = .48, p = .71$ ; GLOB:  $F(3139) = .63, p = .60$ ; LOC:  $F(3139) = .55, p = .65$ ). Therefore, site was not included as a covariate.

Due to protocol changes midway through the study (implemented to address participant motion) the data include three different fMRI run compositions: 113 participants had a single run of 180 volumes; 21 participants had a single run of 156 volumes, and 9 participants had two runs of 116 volumes each which were concatenated into a single 232-volume run. ANOVAs revealed no significant effect of run composition on any of the four network metrics (CPL:  $F(2140) = .546, p = .58$ ; MCC:  $F(2140) = .881, p = .417$ ; GLOB:  $F(2140) = .494, p = .611$ ; LOC:  $F(2140) = 1.19, p = .307$ ). Therefore, fMRI run composition was not included as a covariate.

### Network characteristics of prenatal alcohol exposed (PAE) vs. control participants

As shown in Table 3, there was not a significant group difference in minimum cost to achieve a fully-connected network, [ $t(1141) = .664, p = .51$ ] nor in small-world index (sigma), [ $t(1, 141) = .121, p = .90$ ]. Thus, the graph theory metrics in the following analyses can be considered to represent networks with equivalent parameters across the two groups. Table 3 contains means and effect sizes (Cohen 1992) for the network FC measures with adjacency matrices evaluated at a cost of 0.30. Although MCC was 1.3 % higher in the PAE group compared to the control group, none of the network indices showed a statistically significant difference by group (PAE vs. controls). Thus, at the group level, the network metrics were not sensitive to a simple binary categorization of prenatally exposed vs. non-exposed.

### Examining individuals with atypical network connectivity

Although the network metrics did not distinguish alcohol-exposed children from non-exposed children at the group

level, an alternative approach of examining individuals with atypical network characteristics was undertaken. For each of the four network metrics (CPL, MCC, GLOB, and LOC), grand means and standard deviations were computed for the whole sample (including PAE and controls). For each of the four metrics, individuals were identified as having “typical” (within 1 standard deviation of the grand mean) or “atypical” (outside of 1 standard deviation from the grand mean) network connectivity. Because the intention was to identify individuals with inefficient networks, “atypical” was defined directionally (High CPL, high MCC, and high LOC all represent a “bias” in the network toward highly integrated localized connectivity that is prioritized over efficient long-distance connectivity; low GLOB, similarly, represents a bias toward higher localized connectivity prioritized over more efficient long-distance connectivity). Table 4 shows the distribution of participants with typical and atypical network connectivity. There was a trend-level ( $p = .05$ ) difference for MCC: those with atypically high MCC were 2.4 times more likely to be in the PAE group than in the control group. In addition, there was a significant ( $p = .02$ ) difference for LOC: those with atypically high LOC were 2.7 times more likely to be in the PAE group than in the control group. Applying the Benjamini and Hochberg False Discovery Rate (FDR) correction (Benjamini and Hochberg 1995) to these four analyses results in none of the four null hypotheses being rejected. It should be noted that correcting for this relatively small number of non-independent comparisons that were pre-planned is a conservative approach. The results of the uncorrected analyses remain potentially of interest given the novelty of the data and the consistency with the more robust findings in the next set of sub-group analyses.

### Atypical network connectivity and diagnosis

Out of the 143 participants with good fMRI data, a total of 126 underwent full dysmorphology examinations. The remaining 17 participants did not complete the separate visit for the dysmorphology exam. The dysmorphologist (KLJ) was blind to pre-natal alcohol exposure status (PAE vs. control). Of the 126 examined, 12 (8 %) were identified as FAS, 59 (41 %) were

**Table 3** Group differences in network properties for FASD and control groups at cost = 0.30

Mean $\pm$ SD	PAE ( $n = 75$ )	Control ( $n = 68$ )	Statistic, sig.	% Difference	Cohen's $d$ Effect size
Minimum cost to connect	.146 $\pm$ .06	.140 $\pm$ .06	$t = .664, p = .51$	4.4 %	0.11
Sigma (small world index)	1.57 $\pm$ .16	1.57 $\pm$ .15	$t = .121, p = .90$	0.2 %	0.20
Characteristic Path Length (CPL)	1.85 $\pm$ .06	1.84 $\pm$ .05	$t = .615, p = .54$	0.3 %	0.10
Mean Clustering Coefficient (MCC)	.620 $\pm$ .04	.612 $\pm$ .03	$t = 1.25, p = .21$	1.3 %	0.21
Global Efficiency (GLOB)	.620 $\pm$ .01	.621 $\pm$ .01	$t = .322, p = .75$	0.1 %	0.15
Local Efficiency (LOC)	.800 $\pm$ .02	.795 $\pm$ .02	$t = 1.42, p = .16$	0.6 %	0.24

**Table 4** Distribution of typical and atypical network connectivity for PAE and control participants

n (% within network measure)	PAE (n = 75)	Control (n = 68)	Chi-square, sig.
Characteristic Path Length (CPL)			
Typical	59 (50.9 %)	57 (49.1 %)	$\chi^2 = 0.62, p = .28$
Atypically high	16 (59.3 %)	11 (40.7 %)	
Mean Clustering Coefficient (MCC)			
Typical	56 (48.3 %)	60 (51.7 %)	$\chi^2 = 4.29, p = .05$
Atypically high	19 (70.4 %)	8 (29.6 %)	
Global Efficiency (GLOB)			
Typical	66 (51.6 %)	62 (48.4 %)	$\chi^2 = 0.38, p = .37$
Atypically low	9 (60.0 %)	6 (40.0 %)	
Local Efficiency (LOC)			
Typical	56 (47.9 %)	61 (52.1 %)	$\chi^2 = 5.42, p = .02$
Atypically high	19 (73.1 %)	7 (26.9 %)	

None of the four tests remained statistically significant after applying Benjamini and Hochberg FDR correction

PAE Prenatal Alcohol Exposure

non-FAS, and 55 (39 %) were placed into a “deferred” group. The deferred group contains both participants who have prenatal alcohol exposure ( $n = 37$ ) and participants with no exposure ( $n = 18$ ). As mentioned previously, the deferred group is based on dysmorphology only and reflects the limitations of dysmorphology as applied to the diagnosis of FASD.

A set of analyses focusing on the 55 participants in the deferred group alone reveals that the network FC measures may have potential for further parsing this group in a clinically relevant manner. As shown in Table 5, atypical connectivity was significantly more common among those in the deferred group who were exposed to alcohol vs. those in the deferred group who were not exposed to alcohol. Applying the

Benjamini and Hochberg FDR correction to these data results in rejection of two null hypotheses (LOC and MCC). Three of the metrics (MCC, GLOB, and LOC) were highly specific such that atypical connectivity was seen only in participants with known PAE and not in any without exposure (there were no false positives). Setting a criteria of at least one of these connectivity measures being “atypical” (MCC, GLOB, or LOC), atypical FC identified 15 (27 %) of the original 55 deferred individuals, all of whom were known to have been exposed prenatally to alcohol. No unexposed individuals in the deferred group had atypical connectivity. These analyses demonstrate that network connectivity measures could potentially be used to identify nearly a third of individuals who do not meet criteria

**Table 5** Distribution of typical and atypical network connectivity by prenatal alcohol exposure in a group of 55 children with “deferred” diagnostic status

n (% within network measure)	PAE (n = 37)	Control (n = 18)	Chi-square, sig.
Characteristic Path Length (CPL)			
Typical	28 (63.6 %)	16 (36.4 %)	$\chi^2 = 1.32, p = .307$
Atypically high	9 (81.8 %)	2 (18.2 %)	
Mean Clustering Coefficient (MCC)			
Typical	25 (58.1 %)	18 (41.9 %)	$\chi^2 = 7.47, p = .005$
Atypically high	12 (100 %)	0 (0 %)	
Global Efficiency (GLOB)			
Typical	30 (62.5 %)	18 (37.5 %)	$\chi^2 = 3.90, p = .051$
Atypically low	7 (100 %)	0 (0 %)	
Local Efficiency (LOC)			
Typical	25 (58.1 %)	18 (41.9 %)	$\chi^2 = 7.47, p = .004$
Atypically high	12 (100 %)	0 (0 %)	

After applying Benjamini and Hochberg FDR correction, MCC and LOC remained as statistically significant differences

PAE Prenatal Alcohol Exposure



for FAS, but who clearly have a combination of sub-threshold physical anomalies and neurodevelopmental abnormalities that are specifically related to prenatal alcohol exposure.

### Atypical network connectivity and neurocognitive functioning

A multiple analysis of variance (MANOVA) tested for differences in cognitive ability (global cognitive functioning, memory, and executive functioning) between children with atypical FC and those with typical FC – across the whole sample, including PAE and controls (Table 6). The MANOVA was significant (Wilks' Lambda = .856,  $F(8, 115) = 2.42$ ,  $p = .019$ ). Post-hoc univariate tests revealed that those with atypical connectivity had DAS-II Composite Standard Scores that were 11.4 % lower than those with typical connectivity. There was also a trend-level difference suggesting that verbal memory (NEPSY-II Memory for Names) was lower (13.3 %) in those with atypical connectivity compared to those with typical connectivity. A separate MANOVA, including group (PAE vs. Control), was conducted to determine whether the relationship between cognition and connectivity differed between PAE and Control. The interaction term was not significant [ $F(7114) = .957$ ,  $p = .466$ ].

Across the whole sample, connectivity was associated with global cognitive functioning as illustrated by a Pearson correlation between LOC and DAS-II Composite Standard Score ( $r = -.234$ ,  $p = .005$ ). In these particular data, illustrated in Fig. 1, a 1 % difference in local efficiency (LOC) was associated with a 36.4 point difference in DAS-II Composite Standard Score. Together, these data suggest that the FC metrics examined here may have significant clinical relevance. In a sense, FC abnormalities may serve as “corroborative” evidence, together with neurocognitive deficits, of an underlying neurodevelopmental abnormality in an individual. This could potentially shed light on cases in which the FASD diagnosis is equivocal because of the presence of only minimal dysmorphic features.

### Discussion

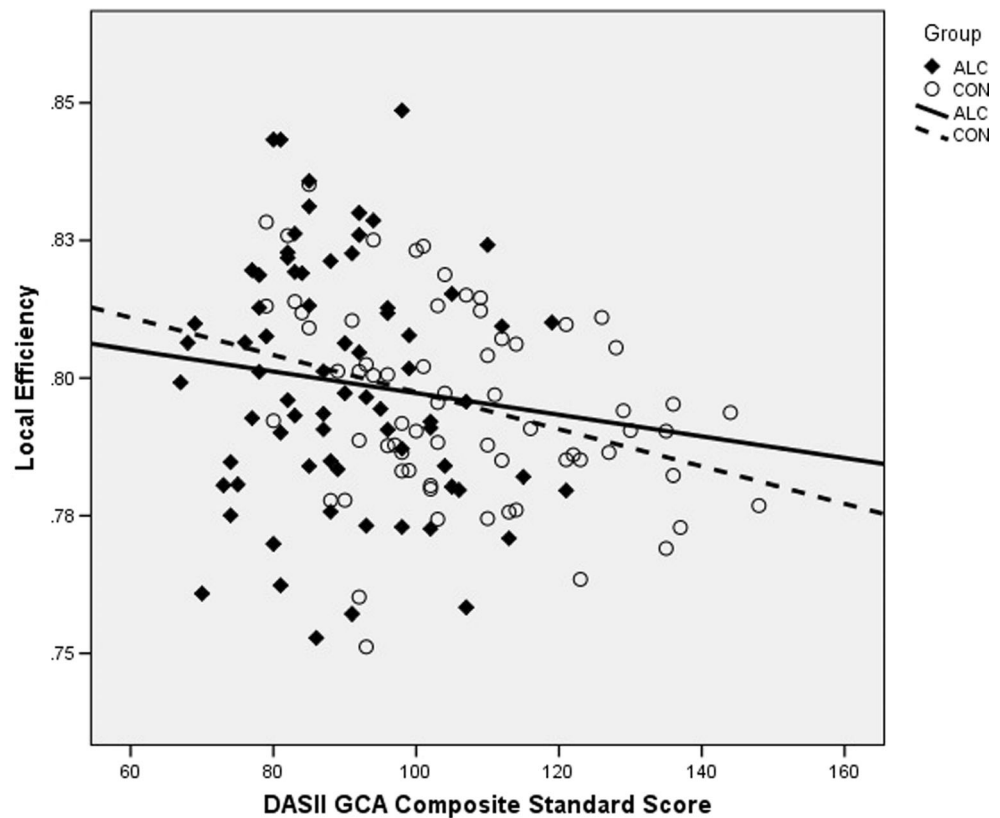
Efficiency in cognitive functioning is dependent on the brain's ability to distribute information processing across its entire network. This distribution allows for the instantaneous “pulling together” of numerous specialized processing centers to meet the demands of the task at hand. Distribution in this manner is also thought to allow for parallel processing, likely increasing efficiency dramatically. Anatomically, the brain's network is comprised of densely connected local processing nodes (cortical and sub-cortical gray matter regions) that are inter-connected over relatively long distances by the network's central backbone – the white matter. Numerous studies have examined the substrate of the network in PAE – using structural and microstructural MRI methods (Donald et al. 2015a, b; Mattson et al. 2013; Wozniak and Muetzel 2011) – in conjunction with assessments of cognition. Here, we examine functional connectivity, gaining new insights into the actual interface between anatomy and cognitive performance.

We have known for some time that PAE damages the hardware that allows the brain to process information efficiently. Some of the earliest studies showed smaller corpus callosum area (Riley et al. 1995), regional white matter hypoplasia (Archibald et al. 2001), altered regional white matter density (Sowell et al. 2001a, b), and callosal shape anomalies in prenatally-exposed subjects (Bookstein et al. 2005; Bookstein et al. 2007; Bookstein et al. 2001; Sowell et al. 2001a, b). More recently, DTI studies have reliably demonstrated alterations in the white matter microstructure in PAE (Donald et al. 2015a, b; Fan et al. 2015; Fryer et al. 2009; Lebel et al. 2010; Lebel et al. 2008; Li et al. 2009; Ma et al. 2005; Malisza et al. 2012; Sowell et al. 2008; Spottiswoode et al. 2011; Taylor et al. 2015; Wozniak et al. 2006; Wozniak et al. 2009). Overall, this body of work suggests that PAE may affect white matter globally rather than regionally, although work continues in this area. A number of existing studies tested for relationships between white matter microstructural abnormalities and physical characteristics of FASD such as

**Table 6** Estimated marginal means, standard deviations (SD), and univariate test results (following MANOVA) for neurocognitive measures

	Typical Connectivity ( $n = 94$ )		Atypical Connectivity ( $n = 30$ )		Univariate tests following MANOVA		
	Mean	SD	Mean	SD	F	p	Effect size (Cohen's $d$ )
DAS-II composite standard score	101.3	17.7	90.4	11.3	10.1	.002*	0.73
CVLT-C trials 1–5 total t-score	50.7	10.6	49.1	11.0	0.5	.481	0.14
NEPSY-II Memory for Designs scaled score	8.9	3.7	8.1	3.5	1.3	.260	0.22
NEPSY-II memory for names scaled score	9.6	3.1	8.4	2.4	3.7	.056	0.43
NEPSY-II narrative memory scales score	9.8	3.5	9.5	3.6	0.2	.690	0.08
NEPSY-II memory for faces scaled score	10.1	2.7	10.8	3.5	1.4	.243	0.22
Trail-making switching scaled score	8.6	3.5	7.9	3.4	1.0	.330	0.20
NEPSY-II inhibition scales score	7.7	3.8	7.2	4.0	0.3	.610	0.13

**Fig. 1** Relationship between local efficiency (LOC) and Differential Ability Scales – Second Edition (DAS-II) Composite Standard Score



dysmorphic facial features. The studies that examined correlations between DTI measures and facial dysmorphology reported no significant relationships (Lebel et al. 2008; Li et al. 2009; Ma et al. 2005; Wozniak et al. 2006; Wozniak et al. 2009), suggesting that these measures may be somewhat independent of each other (i.e. white matter microstructure can be impacted by PAE even when dysmorphic features are not present). White matter integrity has been shown to be associated with cognitive functioning in FASD in a number of domains: executive functioning (Bookstein et al. 2002), inter-hemispheric transfer / finger localization (Roebuck et al. 2002), processing speed (Ma et al. 2005), intelligence (Li et al. 2009), working memory (Malisza, et al. 2012; Wozniak, et al. 2009), and math skill (Lebel et al. 2010). As one would expect from a prenatal insult, white matter disturbances can be detected in the developing fetus (Bookstein, et al. 2005) and have now been shown to be present and measurable with DTI at the newborn stage of life as well (Donald et al. 2015a, b; Taylor et al. 2015).

The existing literature on FC from studies employing fMRI in PAE remains very small at this time and, therefore, the current large-scale examination of FC fills a gap in the literature. Wozniak et al. (2011) initially showed a specific alteration in right-left FC in cortical regions that are heavily interconnected by posterior callosal tracts known to be impacted by PAE. No significant relationship between inter-hemispheric FC and cognitive functioning was observed in

that study, although perceptual reasoning (from the Wechsler Intelligence Scale) was associated with FC at a trend-level. A second study by Wozniak et al. (2013), using a graph theory approach much like the current study, showed network efficiency disadvantages of 1.3 % to 3.5 % for children with PAE compared to controls. Cohen's *d* effect sizes in that study were 0.33 to 0.63 (small to medium effects). The current study showed similar but smaller decrements in network efficiency for those with PAE (0.1 % to 1.3 % and non-significant). The effect sizes were lower in the current study (0.10 to 0.24) (small effects). However, in the current data, a 1 % change in local efficiency was associated with a 36 point change in global cognitive functioning, highlighting the potential importance of small network efficiency differences. Furthermore, the current data also showed that individuals with measurably atypical connectivity were mostly found in the PAE group; they were 2.4–2.7 times more common in the PAE group compared to the control group. Although we do not yet fully know the implications of these types of FC abnormalities, it is thought FC may partly reflect “offline” processing such as memory consolidation and planning (Raichle and Snyder 2007; Tambini et al. 2010). Therefore, disruptions in FC would presumably impact negatively on these important processes in a pervasive manner – i.e. not only when engaged in specific types of tasks.

Resting-state studies, including the current one, show evidence of atypical FC when no task is being performed – the

implication of which is that there are inherent limitations to the network's hardware. Other studies demonstrate that the PAE-affected brain is also inefficient and/or dysfunctional when engaged in specific task performance. For example, Santhanam et al. (2011) showed that engaging in a math task resulted in differences in coupling between two brain networks (the medial-prefrontal cortical network and the posterior cingulate cortical network) for participants with PAE and dysmorphic facial features compared to control participants. They also reported that the cingulum bundle connecting these two nodes of the default mode network had abnormal microstructural characteristics as measured by DTI. Roussotte et al. (2012) showed that individuals with PAE had abnormal FC in corticostriatal networks compared to controls when engaged in a working memory task. Specifically, they observed increased connectivity between putamen and frontal cortex and decreased connectivity between the caudate and frontal cortex in the PAE group.

In the current study, we performed simple group comparisons for the FC measures of interest and found that they were not sufficiently sensitive to discriminate on their own between prenatally exposed and non-exposed individuals. The limitations posed by the methodology and specific analytic decisions may have been a factor in this result. For example, we employed Freesurfer's cortical parcellation which results in ROIs of relatively varied size – some of which are large. Averaging the fMRI signal across relatively large and varied ROIs could have introduced noise into the analyses, making it more difficult to detect a group difference. In the future, an alternative approach might be to employ smaller, more uniform ROIs.

In discussing limitations and caveats to the current study, it is also worth acknowledging that the cutoff we employed for “atypical” connectivity (1 standard deviation) was somewhat arbitrary and a relatively modest cutoff. The cut point was chosen specifically to identify a reasonable number of individuals with atypical connectivity so that relationships with facial dysmorphology and alcohol exposure could be examined. A two standard deviation cutoff would simply have been too restrictive. In addition, the current study defined “atypical” connectivity in a specific direction (High CPL, high MCC, high LOC, and low GLOB all represent a degree of bias in the network toward dense local connectivity prioritized above more efficient long-distance connectivity). Future analyses of the CIFASD dataset, employing more participants, may be able to examine alternative cutoffs. It is also important to note that younger participants were more likely to have been excluded from the study because of in-scanner motion compared to older participants. This finding suggests that future studies may benefit from oversampling younger children or employing additional motion restriction techniques during data collection. Also, it is worth considering that the group distinction employed in this study (PAE vs. control) is not

perfectly precise (we often have imperfect information about amounts of prenatal alcohol exposure, etc.) and, therefore, this imprecision may also have contributed to the lack of an overall main effect of prenatal alcohol exposure on network connectivity measures. Lastly, as in nearly all studies of PAE, we observed high rates of psychiatric co-morbidity in the PAE group compared to the control group. This reflects the reality of the population and cannot realistically be eliminated or controlled, but does need to be considered as important context when interpreting the current results.

Nonetheless, because we observed that atypical FC was much more common in the PAE group compared to controls, we further examined the distribution of atypical FC within the context of other clinical information – in this case, dysmorphic characteristics. In a clinical setting, a pediatric dysmorphologist would apply the diagnostic criteria as was done here, resulting in: 1.) a group diagnosed with FAS; 2.) a group identified as non-FAS; and 3.) a group for which a clear decision could not be made because of only partial diagnostic criteria being present. We examined FC in this sub-group in order to explore whether an objective measure of neurodevelopmental abnormality (atypical FC) would be potentially useful in parsing this heterogeneous group.

For three of the FC metrics, atypical FC was seen only in those who had PAE and not in any of the non-exposed controls in the “deferred” group. Furthermore, atypical FC was shown to be associated with lower global cognitive functioning, also reinforcing its potential clinical relevance. Practically speaking, it remains unlikely that fMRI will ever be utilized in the diagnosis of FASD, but these data suggest that FC metrics may have an important role to play in continuing to push the development of diagnostic criteria and grounding them in neuroscience. One could imagine, for instance, that individual FASD diagnostic criteria or systems of FASD diagnosis could be evaluated against FC metrics and neurocognitive outcomes in order to better understand the strengths and limitations of the criteria and their relevance to outcome. One might also anticipate that FC metrics, such as those presented here, could be used to track developmental changes over time and, potentially, to track changes in network efficiency with cognitive or biological treatments for FASD.

## Conclusion

The current study provides insight into both the limitations and the potential of functional connectivity data in Fetal Alcohol Spectrum Disorders. In this study, whole-brain connectivity metrics proved to be robust (there were no difference across site/scanner nor were there age-related differences) and, thus, potentially useful in the identification of underlying pathology. The data suggest that measures of network integrity / efficiency may help to identify individuals with clear

neurodevelopmental abnormalities among individuals with sub-threshold minor physical anomalies and dysmorphology. Ultimately, although fMRI is not likely to develop into a diagnostic tool itself, this methodology will help to push forward our understanding of how best to identify the full range of individuals impacted by PAE.

**Acknowledgments** This work was performed in conjunction with the Collaborative Initiative on Fetal Alcohol Spectrum Disorders (CIFASD), which is funded by grants from the National Institute on Alcohol Abuse and Alcoholism (NIAAA). Additional information about CIFASD can be found at [www.cifasd.org](http://www.cifasd.org).

#### Compliance with ethical standards

**Funding** This study was funded by the National Institute on Alcohol Abuse and Alcoholism (NIAAA). The following support was utilized in this work: NIAAA U01AA017122 (PI: ERS); NIAAA U01AA14834 (PI: SNM); U24AA014811 (EPR); U24AA014815 (PI: KLJ); U24AA014818 (PI: Barnett); support from the Minnesota Supercomputing Institute.

**Conflict of interest** None of the authors has a relevant conflict of interest to disclose.

**Ethical approval** All procedures performed in studies involving human participants were in accordance with the ethical standards of the institutional and/or national research committee and with the 1964 Helsinki declaration and its later amendments or comparable ethical standards. Informed consent was obtained from all individual participants included in the study. All procedures were reviewed and approved by local human subject's protection programs. This article does not contain any studies with animals performed by any of the authors.

## References

- Achard, S., & Bullmore, E. (2007). Efficiency and cost of economical brain functional networks. *PLoS Comput Biol*, 3(2), e17. doi:10.1371/journal.pcbi.0030017.
- Archibald, S. L., Fennema-Notestine, C., Gamst, A., Riley, E. P., Mattson, S. N., & Jernigan, T. L. (2001). Brain dysmorphology in individuals with severe prenatal alcohol exposure. *Dev Med Child Neurol*, 43(3), 148–154.
- Bassett, D. S., & Bullmore, E. (2006). Small-world brain networks. *Neuroscientist*, 12(6), 512–523.
- Benjamini, Y., & Hochberg, Y. (1995). Controlling the false discovery rate: a practical and powerful approach to multiple testing. *Journal of the Royal Statistical Society*, 57(1), 289–300.
- Biswal, B., Yetkin, F. Z., Haughton, V. M., & Hyde, J. S. (1995). Functional connectivity in the motor cortex of resting human brain using echo-planar MRI. *Magn Reson Med*, 34(4), 537–541.
- Bookstein, F. L., Sampson, P. D., Streissguth, A. P., & Connor, P. D. (2001). Geometric morphometrics of corpus callosum and subcortical structures in the fetal-alcohol-affected brain. *Teratology*, 64(1), 4–32.
- Bookstein, F. L., Sampson, P. D., Connor, P. D., & Streissguth, A. P. (2002). Midline corpus callosum is a neuroanatomical focus of fetal alcohol damage. *Anat Rec*, 269(3), 162–174.
- Bookstein, F. L., Connor, P. D., Covell, K. D., Barr, H. M., Gleason, C. A., Sze, R. W., et al. (2005). Preliminary evidence that prenatal alcohol damage may be visible in averaged ultrasound images of the neonatal human corpus callosum. *Alcohol*, 36(3), 151–160. doi:10.1016/j.alcohol.2005.07.007.
- Bookstein, F. L., Connor, P. D., Huggins, J. E., Barr, H. M., Pimentel, K. D., & Streissguth, A. P. (2007). Many infants prenatally exposed to high levels of alcohol show one particular anomaly of the corpus callosum. *Alcoholism, Clinical and Experimental Research*, 31(5), 868–879. doi:10.1111/j.1530-0277.2007.00367.x.
- Bullmore, E., & Sporns, O. (2009). Complex brain networks: graph theoretical analysis of structural and functional systems. *Nat Rev Neurosci*, 10(3), 186–198. doi:10.1038/nrn2575.
- Cao, W., Li, W., Han, H., O'Leary-Moore, S. K., Sulik, K. K., Allan Johnson, G., et al. (2014). Prenatal alcohol exposure reduces magnetic susceptibility contrast and anisotropy in the white matter of mouse brains. *Neuroimage*, 102(Pt 2), 748–755. doi:10.1016/j.neuroimage.2014.08.035.
- Cohen, J. (1992). A power primer. *Psychological Bulletin*, 112(1), 155–159.
- Dale, A. M., Fischl, B., & Sereno, M. I. (1999). Cortical surface-based analysis. I. Segmentation and surface reconstruction. *Neuroimage*, 9(2), 179–194.
- Delis, D. C., Kramer, J. H., Kaplan, E., & Ober, B. A. (1994). *California Verbal Learning Test Manual, Children's Version*. San Antonio: The Psychological Corporation.
- Delis, D. C., Kaplan, E., & Kramer, J. H. (2001). *Delis-Kaplan Executive Function System (D-KEFS)*. San Antonio, TX: Harcourt Assessment, Inc..
- Donald, K. A., Eastman, E., Howells, F. M., Adnams, C., Riley, E. P., Woods, R. P., et al. (2015a). Neuroimaging effects of prenatal alcohol exposure on the developing human brain: a magnetic resonance imaging review. *Acta Neuropsychiatr*, 27(5), 251–269. doi:10.1017/neu.2015.12.
- Donald, K. A., Roos, A., Fouche, J. P., Koen, N., Howells, F. M., Woods, R. P., et al. (2015b). A study of the effects of prenatal alcohol exposure on white matter microstructural integrity at birth. *Acta Neuropsychiatr*, 27(4), 197–205. doi:10.1017/neu.2015.35.
- Donald, K. A., Ipser, J. C., Howells, F. M., Roos, A., Fouche, J. P., Riley, E. P., et al. (2016). Interhemispheric functional brain connectivity in neonates with prenatal alcohol exposure: preliminary findings. *Alcoholism, Clinical and Experimental Research*, 40(1), 113–121. doi:10.1111/acer.12930.
- Elliott, C. D. (2007). *Differential Ability Scales - Second Edition (DAS-II): Introductory and technical handbook*. San Antonio, TX: PsychCorp.
- Fair, D. A., Cohen, A. L., Power, J. D., Dosenbach, N. U., Church, J. A., Miezin, F. M., et al. (2009). Functional brain networks develop from a "local to distributed" organization. *PLoS Computational Biology*, 5(5), e1000381. doi:10.1371/journal.pcbi.1000381.
- Fan, J., Meintjes, E. M., Moltano, C. D., Spottiswoode, B. S., Dodge, N. C., Alhamud, A. A., et al. (2015). White matter integrity of the cerebellar peduncles as a mediator of effects of prenatal alcohol exposure on eyeblink conditioning. *Human Brain Mapping*, 36(7), 2470–2482. doi:10.1002/hbm.22785.
- Fryer, S. L., Schweinsburg, B. C., Bjorkquist, O. A., Frank, L. R., Mattson, S. N., Spadoni, A. D., et al. (2009). Characterization of white matter microstructure in fetal alcohol spectrum disorders. *Alcoholism, Clinical and Experimental Research*, 33(3), 514–521. doi:10.1111/j.1530-0277.2008.00864.x.
- Green, C. R., Mihic, A. M., Nikkel, S. M., Stade, B. C., Rasmussen, C., Munoz, D. P., et al. (2009). Executive function deficits in children with fetal alcohol spectrum disorders (FASD) measured using the Cambridge neuropsychological tests automated battery (CANTAB). *Journal of Child Psychology and Psychiatry*, 50(6), 688–697. doi:10.1111/j.1469-7610.2008.01990.x.
- Greve, D. N., & Fischl, B. (2009). Accurate and robust brain image alignment using boundary-based registration. *Neuroimage*, 48(1), 63–72. doi:10.1016/j.neuroimage.2009.06.060.



- Jacobson, S. W. (1998). Specificity of neurobehavioral outcomes associated with prenatal alcohol exposure. *Alcoholism, Clinical and Experimental Research*, 22(2), 313–320.
- Jones, K. L., Robinson, L. K., Bakhireva, L. N., Marintcheva, G., Storojev, V., Strahova, A., et al. (2006). Accuracy of the diagnosis of physical features of fetal alcohol syndrome by pediatricians after specialized training. *Pediatrics*, 118(6), E1734–E1738. doi:10.1542/peds.2006-1037.
- Jones, K. L., Hoyme, H. E., Robinson, L. K., Del Campo, M., Manning, M. A., Prewitt, L. M., et al. (2010). Fetal alcohol spectrum disorders: extending the range of structural defects. *American Journal of Medical Genetics. Part A*, 152 A(11), 2731–2735. doi:10.1002/ajmg.a.33675.
- Korkman, M., Kirk, U., & Kemp, S. (2007). *NEPSY-II* (Second ed.). San Antonio, TX: PsychCorp.
- Latora, V., & Marchiori, M. (2001). Efficient behavior of small-world networks. *Phys Rev Lett*, 87(19), 198701.
- Lebel, C., Rasmussen, C., Wyper, K., Walker, L., Andrew, G., Yager, J., et al. (2008). Brain diffusion abnormalities in children with fetal alcohol spectrum disorder. *Alcoholism, Clinical and Experimental Research*, 32(10), 1732–1740. doi:10.1111/j.1530-0277.2008.00750.x.
- Lebel, C., Rasmussen, C., Wyper, K., Andrew, G., & Beaulieu, C. (2010). Brain microstructure is related to math ability in children with fetal alcohol spectrum disorder. *Alcohol Clin Exp Res*, 34(2), 354–363. doi:10.1111/j.1530-0277.2009.01097.x.
- Li, L., Coles, C. D., Lynch, M. E., & Hu, X. (2009). Voxelwise and skeleton-based region of interest analysis of fetal alcohol syndrome and fetal alcohol spectrum disorders in young adults. *Hum Brain Mapp*, 30(10), 3265–3274.
- Ma, X., Coles, C. D., Lynch, M. E., Laconte, S. M., Zurkiya, O., Wang, D., et al. (2005). Evaluation of corpus callosum anisotropy in young adults with fetal alcohol syndrome according to diffusion tensor imaging. *Alcoholism, Clinical and Experimental Research*, 29(7), 1214–1222.
- Malisza, K. L., Buss, J. L., Bolster, R. B., de Gervai, P. D., Woods-Frohlich, L., Summers, R., et al. (2012). Comparison of spatial working memory in children with prenatal alcohol exposure and those diagnosed with ADHD: a functional magnetic resonance imaging study. *Journal of Neurodevelopmental Disorders*, 4(1). doi:10.1186/1866-1955-4-12.
- Mattson, S. N., Riley, E. P., Gramling, L., Delis, D. C., & Jones, K. L. (1997). Heavy prenatal alcohol exposure with or without physical features of fetal alcohol syndrome leads to IQ deficits. *J Pediatr*, 131(5), 718–721.
- Mattson, S. N., Foroud, T., Sowell, E. R., Jones, K. L., Coles, C. D., Fagerlund, A., et al. (2010). Collaborative initiative on fetal alcohol spectrum disorders: methodology of clinical projects. *Alcohol*, 44(7–8), 635–641. doi:10.1016/j.alcohol.2009.08.005.
- Mattson, S. N., Roesch, S. C., Glass, L., Deweese, B. N., Coles, C. D., Kable, J. A., et al. (2013). Further development of a neurobehavioral profile of fetal alcohol spectrum disorders. *Alcoholism, Clinical and Experimental Research*, 37(3), 517–528. doi:10.1111/j.1530-0277.2012.01952.x.
- Power, J. D., Barnes, K. A., Snyder, A. Z., Schlaggar, B. L., & Petersen, S. E. (2012). Spurious but systematic correlations in functional connectivity MRI networks arise from subject motion. *Neuroimage*, 59(3), 2142–2154. doi:10.1016/j.neuroimage.2011.10.018.
- Raichle, M. E., & Snyder, A. Z. (2007). A default mode of brain function: a brief history of an evolving idea. *Neuroimage*, 37(4), 1083–1090 discussion 1097–1089.
- Riley, E. P., Mattson, S. N., Sowell, E. R., Jernigan, T. L., Sobel, D. F., & Jones, K. L. (1995). Abnormalities of the corpus callosum in children prenatally exposed to alcohol. *Alcohol Clin Exp Res*, 19(5), 1198–1202.
- Riley, E. P., McGee, C. L., & Sowell, E. R. (2004). Teratogenic effects of alcohol: a decade of brain imaging. *Am J Med Genet C Semin Med Genet*, 127(1), 35–41.
- Roebuck, T. M., Mattson, S. N., & Riley, E. P. (2002). Interhemispheric transfer in children with heavy prenatal alcohol exposure. *Alcohol Clin Exp Res*, 26(12), 1863–1871.
- Roussotte, F. F., Rudie, J. D., Smith, L., O'Connor, M. J., Bookheimer, S. Y., Narr, K. L., et al. (2012). Frontostriatal connectivity in children during working memory and the effects of prenatal methamphetamine, alcohol, and Polydrug exposure. *Developmental Neuroscience*, 34(1), 43–57. doi:10.1159/000336242.
- Rubinov, M., & Sporns, O. (2010). Complex network measures of brain connectivity: uses and interpretations. *Neuroimage*, 52(3), 1059–1069. doi:10.1016/j.neuroimage.2009.10.003.
- Santhanam, P., Coles, C. D., Li, Z., Li, L., Lynch, M. E., & Hu, X. (2011). Default mode network dysfunction in adults with prenatal alcohol exposure. *Psychiatry Res*, 194(3), 354–362. doi:10.1016/j.psychres.2011.05.004.
- Shaffer, D., Fisher, P., Lucas, C. P., Dulcan, M. K., & Schwab-Stone, M. E. (2000). NIMH Diagnostic Interview Schedule for Children Version IV (NIMH DISC-IV): description, differences from previous versions, and reliability of some common diagnoses. *J Am Acad Child Adolesc Psychiatry*, 39(1), 28–38. doi:10.1097/00004583-200001000-00014.
- Smith, S. M., Jenkinson, M., Woolrich, M. W., Beckmann, C. F., Behrens, T. E., Johansen-Berg, H., et al. (2004). Advances in functional and structural MR image analysis and implementation as FSL. *Neuroimage*, 23(Suppl 1), S208–S219. doi:10.1016/j.neuroimage.2004.07.051.
- Sowell, E. R., Mattson, S. N., Thompson, P. M., Jernigan, T. L., Riley, E. P., & Toga, A. W. (2001a). Mapping callosal morphology and cognitive correlates: Effects of heavy prenatal alcohol exposure. *Neurology*, 57(2), 235–244.
- Sowell, E. R., Thompson, P. M., Mattson, S. N., Tessner, K. D., Jernigan, T. L., Riley, E. P., et al. (2001b). Voxel-based morphometric analyses of the brain in children and adolescents prenatally exposed to alcohol. *Neuroreport*, 12(3), 515–523.
- Sowell, E. R., Johnson, A., Kan, E., Lu, L. H., Van Horn, J. D., Toga, A. W., et al. (2008). Mapping white matter integrity and neurobehavioral correlates in children with fetal alcohol spectrum disorders. *The Journal of Neuroscience*, 28(6), 1313–1319. doi:10.1523/JNEUROSCI.5067-07.2008.
- Sowell, E. R., Leow, A. D., Bookheimer, S. Y., Smith, L. M., O'Connor, M. J., Kan, E., et al. (2010). Differentiating prenatal exposure to methamphetamine and alcohol versus alcohol and not methamphetamine using tensor-based brain morphometry and discriminant analysis. *The Journal of Neuroscience*, 30(11), 3876–3885. doi:10.1523/JNEUROSCI.4967-09.2010.
- Spottiswoode, B. S., Meintjes, E. M., Anderson, A. W., Molteni, C. D., Stanton, M. E., Dodge, N. C., et al. (2011). Diffusion tensor imaging of the cerebellum and eyeblink conditioning in fetal alcohol spectrum disorder. *Alcoholism, Clinical and Experimental Research*, 35(12), 2174–2183. doi:10.1111/j.1530-0277.2011.01566.x.
- Streissguth, A. P., & O'Malley, K. (2000). Neuropsychiatric implications and long-term consequences of fetal alcohol spectrum disorders. *Semin Clin Neuropsychiatry*, 5(3), 177–190.
- Tambini, A., Ketz, N., & Davachi, L. (2010). Enhanced brain correlations during rest are related to memory for recent experiences. *Neuron*, 65(2), 280–290. doi:10.1016/j.neuron.2010.01.001.
- Taylor, P. A., Jacobson, S. W., van der Kouwe, A., Molteni, C. D., Chen, G., Wintermark, P., et al. (2015). A DTI-based tractography study of effects on brain structure associated with prenatal alcohol exposure in newborns. *Human Brain Mapping*, 36(1), 170–186. doi:10.1002/hbm.22620.
- Watts, D. J., & Strogatz, S. H. (1998). Collective dynamics of 'small-world' networks. *Nature*, 393(6684), 440–442. doi:10.1038/30918.

- Woolrich, M. W., Jbabdi, S., Patenaude, B., Chappell, M., Makni, S., Behrens, T., et al. (2009). Bayesian analysis of neuroimaging data in FSL. *Neuroimage*, *45*(1 Suppl), S173–S186. doi:10.1016/j.neuroimage.2008.10.055.
- Wozniak, J. R., & Muetzel, R. L. (2011). What does diffusion tensor imaging reveal about the brain and cognition in fetal alcohol spectrum disorders? *Neuropsychology Review*, *21*(2), 133–147. doi:10.1007/s11065-011-9162-1.
- Wozniak, J. R., Mueller, B. A., Chang, P. N., Muetzel, R. L., Caros, L., & Lim, K. O. (2006). Diffusion tensor imaging in children with fetal alcohol spectrum disorders. *Alcohol Clin Exp Res*, *30*, 1799–1806. doi:10.1111/j.1530-0277.2006.00213.x.
- Wozniak, J. R., Muetzel, R. L., Mueller, B. A., McGee, C. L., Freerks, M. A., Ward, E. E., et al. (2009). Microstructural corpus callosum anomalies in children with prenatal alcohol exposure: an extension of previous diffusion tensor imaging findings. *Alcoholism, Clinical and Experimental Research*, *33*(10), 1825–1835. doi:10.1111/j.1530-0277.2009.01021.x.
- Wozniak, J. R., Mueller, B. A., Muetzel, R. L., Bell, C. J., Hoecker, H. L., Nelson, M. L., et al. (2011). Inter-hemispheric functional connectivity disruption in children with prenatal alcohol exposure. *Alcoholism, Clinical and Experimental Research*, *35*(5), 849–861. doi:10.1111/j.1530-0277.2010.01415.x.
- Wozniak, J. R., Mueller, B. A., Bell, C. J., Muetzel, R. L., Hoecker, H. L., Boys, C. J., et al. (2013). Global functional connectivity abnormalities in children with fetal alcohol spectrum disorders. *Alcoholism, Clinical and Experimental Research*, *37*(5), 748–756. doi:10.1111/acer.12024.
- Wu, K., Taki, Y., Sato, K., Hashizume, H., Sassa, Y., Takeuchi, H., et al. (2013). Topological organization of functional brain networks in healthy children: differences in relation to age, sex, and intelligence. *PLoS One*, *8*(2), e55347. doi:10.1371/journal.pone.0055347.